Improved Model-Independent Analysis of Semileptonic and Radiative Rare B Decays

Enrico Lunghi*†

Insitut für Theoretische Physik, Univerität Zürich, 8057 Zürich, Switzerland

Abstract

We study the impact of recent B-factories measurements and upper limit of radiative and semileptonic rare B-decays. We present model independent constraints on the relevant Wilson coefficients and show the impact on the parameter space of some concrete realizations of the Minimal Supersymmetric Standard Model.

1 Experimental inputs

In this talk we use the most recent experimental results on inclusive and exclusive $b \to s\gamma$ and $b \to s\ell^+\ell^-$ decays to update the analysis presented in Ref. [1]. The experimental results that we use in the analysis are

$$\begin{aligned}
\mathcal{B}(B \to X_s\gamma) &= (3.40^{+0.42}_{-0.37}) \times 10^{-4} \text{ [2–5]}, && (1)\\
\mathcal{B}(B \to K\ell^+\ell^-) &= (0.63^{+0.14}_{-0.13}) \times 10^{-6} \text{ [6,7]}, && (2)\\
\mathcal{B}(B \to K^*\mu^+\mu^-) &\leq 3.0 \times 10^{-6} \text{ at 90\% C.L. [6,7]}, && (3)\\
\mathcal{B}(B \to K^*e^+e^-) &= (1.68^{+0.68}_{-0.58} \pm 0.28) \times 10^{-6} \text{ [6]}, && (4)\\
\mathcal{B}(B \to X_s\mu^+\mu^-) &= (7.9 \pm 2.1^{+2.0}_{-1.5}) \times 10^{-6} \text{ [8]}, && (5)\\
\mathcal{B}(B \to X_se^+e^-) &= (5.0 \pm 2.3^{+1.2}_{-1.1}) \times 10^{-6} \text{ [8]}, && (6)\\
\mathcal{B}(B \to X_s\ell^+\ell^-) &= (6.1 \pm 1.4^{+1.3}_{-1.1}) \times 10^{-6} \text{ [8]}. && (7)
\end{aligned}$$

The $B \to X_s\gamma$ branching ratio is given with a cut on the photon energy ($E_\gamma > m_b/20$) and the value presented is the weighted average of the four available measurements. The branching ratios for the semileptonic modes (2–7) refer to the non–resonant branching ratios integrated over the dilepton invariant mass spectrum. On the theoretical side, this amounts to consider only the perturbative part of the amplitude and to leave out all the resonant contributions (that are usually shaped using Breit-Wigner ansätze). On the experimental one, judicious cuts are used to remove the dominant resonant contributions arising from intermediate $c\bar{c}$ resonances ($J/\psi, \psi', ...$); SM-based theoretical distributions [9] are then used to correct the data for the experimental acceptance. Finally, let us stress that the $B \to X_se^+e^-$ branching ratio is given with a cut on the di-lepton invariant mass, $M_{ee} \equiv \sqrt{s} > 0.2$ GeV, in order to remove virtual photon contributions and the $\pi^0 \to ee\gamma$ photon conversion background. The $B \to X_se^+e^-$ rate increases steeply for $s \to 0$ (because of the almost real photon pole) and is extremely sensitive to the Wilson coefficient of the magnetic moment operator (that controls the $b \to s\gamma$ transition). The

*E-mail address: lunghi@mail.desy.de

†This work is supported by the Swiss National Fond

use of the branching ratio without extrapolation to the full s spectrum, allows to reduce the uncertainties in the comparison with the Standard Model (SM) prediction and to properly analyze models with an enhanced magnetic moment Wilson coefficient.

2 Theoretical framework and SM predictions

The effective Hamiltonian in the SM inducing the $b \to s\ell^+\ell^-$ and $b \to s\gamma$ transitions is (up to negligible contributions proportional to $V_{us}^* V_{ub}$)

$$\mathcal{H}_{\rm eff} = -\frac{4G_F}{\sqrt{2}} V_{ts}^* V_{tb} \sum_{i=1}^{10} C_i(\mu)\, O_i(\mu) \quad , \tag{8}$$

where G_F is the Fermi constant and V_{ij} are the CKM matrix elements. $O_i(\mu)$ are dimension-six operators at the scale μ and $C_i(\mu)$ are the corresponding Wilson coefficients. The most relevant operators are (the complete list can be found, for instance, in Ref. [1])

$$O_7 = \frac{e}{g_s^2} m_b (\bar{s}_L \sigma^{\mu\nu} b_R) F_{\mu\nu} \,, \tag{9}$$

$$O_8 = \frac{1}{g_s} m_b (\bar{s}_L \sigma^{\mu\nu} T^a b_R) G^a_{\mu\nu} \,, \tag{10}$$

$$O_9 = \frac{e^2}{g_s^2} (\bar{s}_L \gamma_\mu b_L) \sum_\ell (\bar{\ell} \gamma^\mu \ell) \,, \tag{11}$$

$$O_{10} = \frac{e^2}{g_s^2} (\bar{s}_L \gamma_\mu b_L) \sum_\ell (\bar{\ell} \gamma^\mu \gamma_5 \ell) \,, \tag{12}$$

where the subscripts L and R refer to left- and right- handed components of the fermion fields.

The differential decay width for the inclusive decay $B \to X_s \ell^+ \ell^-$ is given by the parton level result supplement by calculable power corrections. In the NNLO approximation, the non–resonant decay width can be written as

$$\frac{d\Gamma(b \to s\ell^+\ell^-)}{d\hat{s}} = \left(\frac{\alpha_{em}}{4\pi}\right)^2 \frac{G_F^2 m_{b,pole}^5 \left|V_{ts}^* V_{tb}\right|^2}{48\pi^3} (1-\hat{s})^2 \left[(1+2\hat{s}) \left(\left|\widetilde{C}_9^{\rm eff}\right|^2 + \left|\widetilde{C}_{10}^{\rm eff}\right|^2 \right) G_1(\hat{s}) \right.$$
$$\left. + 4\,(1+2/\hat{s}) \left|\widetilde{C}_7^{\rm eff}\right|^2 G_2(\hat{s}) + 12{\rm Re}\left(\widetilde{C}_7^{\rm eff} \widetilde{C}_9^{\rm eff *} \right) G_3(\hat{s}) + G_c(\hat{s}) \right] \,, \tag{13}$$

where $\hat{s} \equiv s/m_b^2$ and the functions $G_i(\hat{s})$ $(i = 1, 2, 3)$ and $G_c(\hat{s})$ encode respectively the $1/m_b^2$ and $1/m_c^2$ corrections. $\widetilde{C}_i^{\rm eff}$ are effective Wilson coefficients (whose explicit form is given in Ref. [1]) that are functions of the dilepton mass squared and incorporate part of the operator matrix elements. In particular, $\widetilde{C}_9^{\rm eff}$ contains contributions due to perturbative $c\bar{c}$ rescattering and develops an imaginary part for $s > 4m_c^2$. Performing the

$\hat{s}$ integration and constraining $s_{ee} > (0.2\ \text{GeV})^2$, the decay widths in electrons and muons are essentially equal and are given by the following numerical formula:

$$\mathcal{B}(B \to X_s \ell^+ \ell^-) = \Big[4.534 + 8.665\ |C_7^{\rm tot}|^2 + .119\ (|C_9^{\rm NP}|^2 + |C_{10}^{\rm NP}|^2) + .996\ {\rm Re}\, C_7^{\rm tot} C_9^{\rm NP*} \\ +4.130\ {\rm Re}\, C_7^{\rm tot} + 0.171\ {\rm Im}\, C_7^{\rm tot} + 1.068\ {\rm Re}\, C_9^{\rm NP} + .064\ {\rm Im}\, C_9^{\rm NP} - 1.011\ {\rm Re}\, C_{10}^{\rm NP}\Big] \times 10^{-6}\,,$$

where $C_9^{\rm NP}$ and $C_{10}^{\rm NP}$ are the new physics contributions to $C_9(\mu_W)$ and $C_{10}(\mu_W)$ evaluated at $\mu_W \simeq m_W$ and $C_7^{\rm tot}$ is the sum of the SM ($C_7^{\rm SM}(\mu_b)$) and new physics ($C_7^{\rm NP}(\mu_b)$) contributions evaluated at $\mu_b \simeq 2.5$ GeV. A detailed discussion of all the assumptions that enter this formula can be found in Ref. [1]. In the SM we find

$$\mathcal{B}(B \to X_s \ell^+ \ell^-) = (4.15 \pm 0.27 \pm 0.21 \pm 0.62) \times 10^{-6} = (4.15 \pm 0.70) \times 10^{-6} \qquad (14)$$

where the errors correspond to variations of μ_b, $m_{t,pole}$ and m_c/m_b. Comparing this estimate with the experimental measurements (5)–(7) we see that there is agreement with the SM at the 1 σ level. Note that Previous experimental data on the di-electron channel were extrapolated using SM-based distributions and that the branching ratio for $B \to X_s e^+ e^-$ integrated over the whole dilepton invariant mass spectrum is [1] $(6.89 \pm 1.01) \times 10^{-6}$ (i.e. the $s_{ee} < (0.2\ \text{GeV})^2$ region enhances (14) by 66%). This clearly shows to what extent the choice to give branching ratios not extrapolated allows for a cleaner identification of new physics effects.

For what concerns the exclusive decays $B \to K^{(*)} \ell^+ \ell^-$, we implement the NNLO corrections calculated by Bobeth et al. in Ref. [10] and by Asatrian et al. in Ref. [11] for the short-distance contribution. Then, we use the form factors calculated with the help of the QCD sum rules in Ref. [12]. For lack of space we can not describe some subtleties related to the treatment of the so–called hard spectator interactions and to the value of the magnetic moment form factor at $s = 0$ (see Ref. [1] for a complete discussion). The SM NNLO predictions that we obtain are

$$\mathcal{B}(B \to K \ell^+ \ell^-) = (0.35 \pm 0.12) \times 10^{-6} \quad (\delta\mathcal{B}_{K\ell\ell} = \pm 34\%)\,, \qquad (15)$$

$$\mathcal{B}(B \to K^* e^+ e^-) = (1.58 \pm 0.49) \times 10^{-6} \quad (\delta\mathcal{B}_{K^*ee} = \pm 31\%)\,, \qquad (16)$$

$$\mathcal{B}(B \to K^* \mu^+ \mu^-) = (1.19 \pm 0.39) \times 10^{-6} \quad (\delta\mathcal{B}_{K^*\mu\mu} = \pm 33\%)\,. \qquad (17)$$

From the comparison with Eqs. (2)–(3) we see that in the $B \to K \ell^+ \ell^-$ channel there is a 1.6 σ discrepancy with the SM expectation while in the K^* channels there is a perfect agreement.

3 Model independent analysis

The first step consists in extracting the bounds that the measurement (1) implies for $C_7^{\rm tot}(2.5\ \text{GeV})$. The main difficulty arises from the treatment of the m_c dependence of the $B \to X_s \gamma$ branching ratio. In Ref. [13], it was noted that, in this decay, the charm quark mass enters the matrix elements at the two-loop level only and that it would be more appropriate to use the running charm mass evaluated at the $\mu_b \simeq O(m_b)$ scale, leading

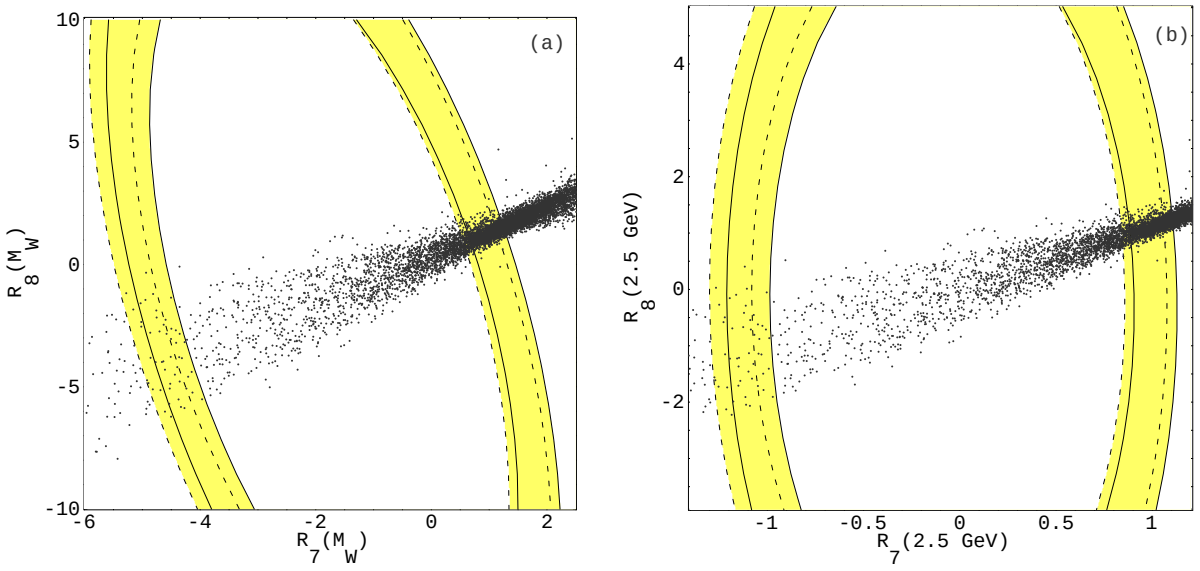

Figure 1: 90% C.L. *bounds in the* $[R_7(\mu), R_8(\mu)]$ *plane following from the world average* $B \to X_s\gamma$ *branching ratio for* $\mu = m_W$ *(left-hand plot) and* $\mu = 2.5$ *GeV (right-hand plot). Theoretical uncertainties are taken into account. The solid and dashed lines correspond to the* $m_c = m_{c,pole}$ *and* $m_c = \overline{m_c^{MS}}(\mu_b)$ *cases respectively. The scatter points correspond to the expectation in MFV models.*

to $m_c/m_b \simeq 0.22 \pm 0.04$, compared to $m_{c,pole}/m_b \simeq 0.29 \pm 0.02$. This is a reasonable choice since the charm quark enters only as virtual particle running inside loops; formally, on the other hand, it is also clear that the difference between the results obtained by interpreting m_c as the pole mass or the running mass is formally a NNLO effect. In what concerns $b \to s\ell^+\ell^-$, the situation is somewhat different, as the charm quark mass enters in this case also in some one-loop matrix elements. In these one-loop contributions, m_c has the meaning of the pole mass when using the expressions derived in Ref. [11]. Since the bounds on the C_7 do not depend dramatically on m_c, we just derive them using both values of the charm mass and taking the union of the allowed ranges. We present the results of this analysis in Figs. 1a and 1b, where we show the allowed regions in the R_7 and R_8 plane obtained using the 90% C.L. $B \to X_s\gamma$ bound (here $R_{7,8} \equiv C_{7,8}^{\rm tot}/C_{7,8}^{\rm SM}$). We take $|R_8(\mu_W)| \leq 10$ in order to satisfy the constraints from the decays $b \to sg$ and $B \to X_q$ [14].The regions in Fig. 1b translate in the following allowed constraints:

$$\begin{cases} m_c/m_b = 0.29: & C_7^{\rm tot}(2.5\ {\rm GeV}) \in [-0.37, -0.18]\ \&\ [0.21, 0.40]\ , \\ m_c/m_b = 0.22: & C_7^{\rm tot}(2.5\ {\rm GeV}) \in [-0.35, -0.17]\ \&\ [0.25, 0.43]\ . \end{cases} \tag{18}$$

In the subsequent numerical analysis we impose the union of the above allowed ranges

$$-0.37 \leq C_7^{{\rm tot},<0}(2.5\ {\rm GeV}) \leq -0.17 \quad \& \quad 0.21 \leq C_7^{{\rm tot},>0}(2.5\ {\rm GeV}) \leq 0.43 \tag{19}$$

calling them $C_7^{\rm tot}$–positive and $C_7^{\rm tot}$–negative solutions.

We present the results of the model independent analysis of $b \to s\ell^+\ell^-$ decays in Fig. 2. Within each plot we vary $C_7^{\rm tot}$ inside the allowed ranges (19) and plot the 90% C.L.

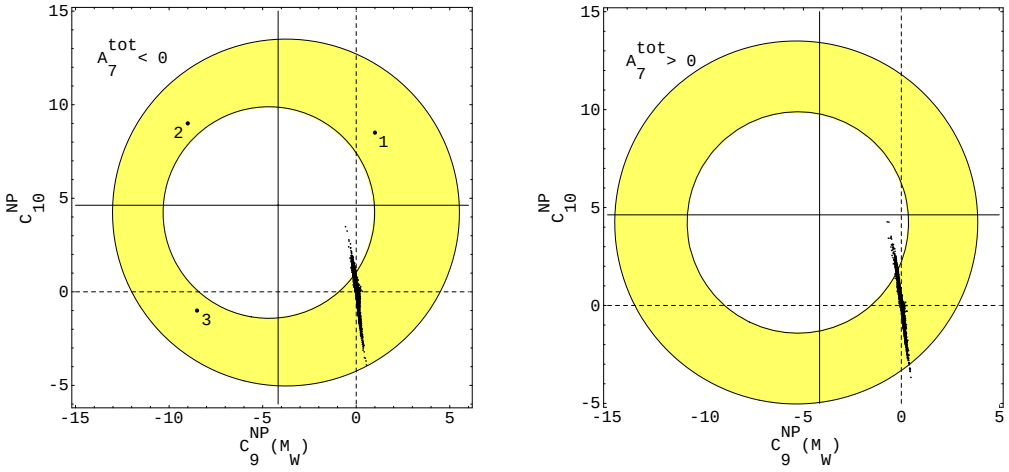

Figure 2: **NNLO Case.** *Constraints on new physics contributions to the Wilson coefficients C_9 and C_{10} implied by $b \to s\ell^+\ell^-$ decays. The plots correspond to the $C_7^{\rm tot}(2.5\ GeV) < 0$ and $C_7^{\rm tot}(2.5\ GeV) > 0$ case, respectively. The points are obtained by means of a scanning over the EMFV parameter space and requiring the experimental bound from $B \to X_s\gamma$ to be satisfied.*

constraints implied by Eqs. (2)–(7) in the $[C_9^{\rm NP}(\mu_W), C_{10}^{\rm NP}]$ plane. The SM correspond to the point (0,0). In each plot the inner and outer contours are determined by the measurements of the decays $B \to K\ell^+\ell^-$ and $B \to X_s\ell^+\ell^-$ respectively.

4 Analysis in supersymmetry

In this section we analyze the impact that the measurements (1)–(7) have on three variants of the minimal supersymmetric standard model (MSSM), namely minimal flavour violation (MFV), gluino mediated contributions and extended minimal flavour violation (EMFV).

MFV. As already known from the existing literature (see for instance Ref. [15]), minimal flavour violating contributions are generally too small to produce sizable effects on the Wilson coefficients C_9 and C_{10}. Indeed, scanning over the MFV parameter space and imposing the lower bounds on the sparticle masses we obtain

$$C_7^{\rm tot} < 0 : \begin{cases} C_9^{MFV}(\mu_W) \in [-0.2, 0.4] \\ C_{10}^{MFV} \in [-1.0, 0.7] \end{cases}, \quad C_7^{\rm tot} > 0 : \begin{cases} C_9^{MFV}(\mu_W) \in [-0.2, 0.3] \\ C_{10}^{MFV} \in [-0.8, 0.5] \end{cases}. \quad (20)$$

From the comparison of the size of these contributions with the allowed regions depicted in Fig. 2 we see that the current experimental results on $b \to s\ell^+\ell^-$ decays are not precise enough to constraint the MFV parameter space. The situation is completely different for what concerns $b \to s\gamma$. The scatter plot presented in Fig. 1 is obtained varying the MFV SUSY parameters and shows the strong correlation between the values of the Wilson

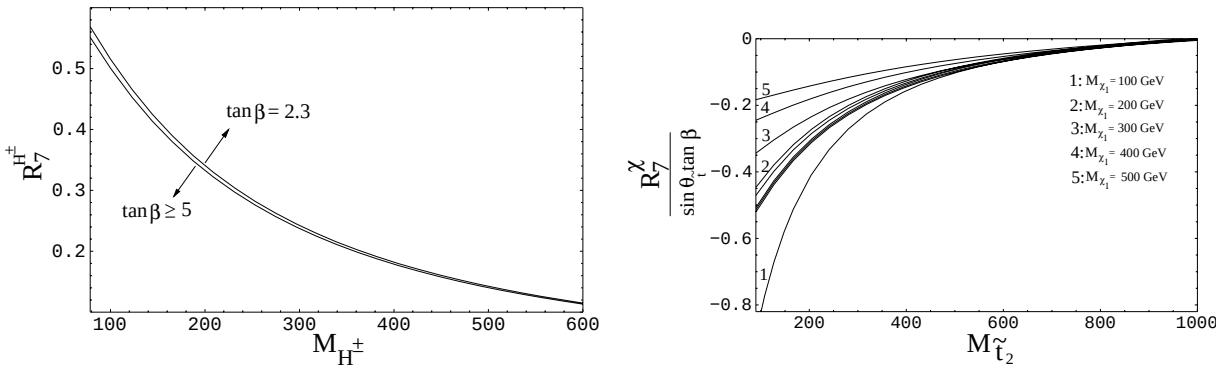

Figure 3: **Left plot:** *Dependence of* $R_7^{H^\pm}(\mu_b) \equiv C_7^{H^\pm}(\mu_b)/C_7^{\rm SM}(\mu_b)$ *on the mass of the charged Higgs.* **Right plot:** *Dependence of* $R_7^{\chi}(\mu_b) \equiv C_7^{\chi}(\mu_b)/C_7^{\rm SM}(\mu_b)$ *on the mass of the lightest stop in MFV models. The chargino contribution is essentially proportional to* $\sin\theta_{\tilde{t}}\tan\beta$ *for not too small* $\sin\theta_{\tilde{t}}$*. For the curve 2 we show the variation due to several choices of* $\theta_{\tilde{t}}$ *and* $\tan\beta$*.*

coefficients C_7 and C_8. In fact, the SUSY contributions to the magnetic and chromo–magnetic coefficients differ only because of colour factors and loop-functions. In Fig. 3 we present, finally, the dependence of the charged Higgs and chargino contributions to C_7 on the relevant mass parameters (that are the charged Higgs mass for the former and the lightest chargino and stop masses for the latter). From these figures is clear that the knowledge of the sign of $C_7^{\rm tot}$ will strongly constrain the MFV parameter space, by putting upper or lower limits on the chargino and stop masses.

Gluino contributions. Gluino contributions to C_9 and C_{10} are governed by mass insertions in the down squark mass matrix. From the analysis presented in Ref. [15] we see that the dominant diagrams involve the parameter $(\delta^d_{23})_{LL}$ and that large deviations from the SM are unlikely.

Extended–MFV models. A basically different scenario arises if chargino–mediated penguin and box diagrams are considered. As can be inferred by Table 4 in Ref. [15], the presence of a light $\tilde{t}_2$ generally gives rise to large contributions to C_9 and especially to C_{10}. EMFV models are based on the heavy squarks and gluino assumption. In this framework, the charged Higgs and the lightest chargino and stop masses are required to be heavier than 100 GeV in order to satisfy the lower bounds from direct searches. The rest of the SUSY spectrum is assumed to be almost degenerate and heavier than 1 TeV. The lightest stop is almost right–handed and the stop mixing angle (which parameterizes the amount of the left-handed stop $\tilde{t}_L$ present in the lighter mass eigenstate) turns out to be of order $O(m_W/M_{\tilde{q}}) \simeq 10\%$. The assumption of a heavy ($\geq$ 1 TeV) gluino totally suppresses any possible gluino–mediated SUSY contribution to low energy observables. Note that even in the presence of a light gluino (i.e. $M_{\tilde{g}} \simeq O(300$ GeV)) these penguin diagrams remain suppressed due to the heavy down squarks present in the loop. In the MIA approach, a diagram can contribute sizeably only if the inserted mass insertions involve the light stop. All the other diagrams require necessarily a loop with at least two heavy ($\geq$ 1 TeV) squarks and are therefore automatically suppressed. This leaves

us with only two unsuppressed flavour changing sources other than the CKM matrix, namely the mixings $\tilde{u}_L - \tilde{t}_2$ (denoted by $\delta_{\tilde{u}_L\tilde{t}_2}$) and $\tilde{c}_L - \tilde{t}_2$ (denoted by $\delta_{\tilde{c}_L\tilde{t}_2}$). We note that $\delta_{\tilde{u}_L\tilde{t}_2}$ and $\delta_{\tilde{c}_L\tilde{t}_2}$ are mass insertions extracted from the up–squarks mass matrix after the diagonalization of the stop system and are therefore linear combinations of $(\delta_{13})^U_{LR}$, $(\delta_{13})^U_{LL}$ and of $(\delta_{23})^U_{LR}$, $(\delta_{23})^U_{LL}$, respectively. In Fig. 2 we present the results of an high statistic scanning over the EMFV parameter space requiring each point to survive the constraints coming from the sparticle masses lower bounds and $b \to s\gamma$. Note that these SUSY models can account only for a small part of the region allowed by the model independent analysis of current data. In the numerical analysis reported here, we have used the integrated branching ratios alone to put constraints on the effective coefficients. This procedure allows multiple solutions, which can be disentangled from each other only with the help of both the dilepton mass spectra and the forward-backward asymmetries. Only such measurements would allow us to determine the exact values and signs of the Wilson coefficients C_7, C_9 and C_{10}.

References

[1] A. Ali, C, Greub, G, Hiller, E. Lunghi, Phys. Rev. D**66** (2002) 034002.

[2] R. Barate *et al.* (ALEPH Collaboration), Phys. Lett. B**421** (1998) 169.

[3] D. Chen *et al.* (CLEO Collaboration), Phys. Rev. Lett. **87** (2001) 251807.

[4] B. Aubert *et al.* (BABAR Collaboration), hep-ex/0207076.

[5] K. Abe *et al.* (BELLE Collaboration), Phys. Lett B**511** (2001) 151.

[6] B. Aubert *et al.* (BABAR Collaboration), hep-ex/0207082.

[7] K. Abe *et al.* (BELLE Collaboration), BELLE-CONF-0241.

[8] J. Kaneko *et al.* [Belle Collaboration], hep-ex/0208029.

[9] A. Ali, G. Hiller, L. T. Handoko and T. Morozumi, Phys. Rev. D**55** (1997) 4105;
A. Ali, P. Ball, L. T. Handoko and G. Hiller, Phys. Rev. D**61** (2000) 074024.

[10] C. Bobeth, M. Misiak and J. Urban, Nucl. Phys. B**574** (2000) 291.

[11] H. H. Asatrian, H. M. Asatrian, C. Greub, M. Walker, Phys. Lett B**507** (2001) 162;
H. H. Asatryan, H. M. Asatrian, C. Greub, M. Walker, Phys. Rev. D**65** (2002) 074004.

[12] A. Ali, P. Ball, L. T. Handoko and G. Hiller, Phys. Rev. D**61** (2000) 074024.

[13] P. Gambino and M. Misiak, Nucl. Phys. B**611** (2001) 338.

[14] C. Greub and P. Liniger, Phys. Rev. D**63** (2001) 054025.

[15] E. Lunghi, A. Masiero, I. Scimemi and L. Silvestrini, Nucl. Phys. B**568** (2000) 120.